Received: 21 November 2017 | Revised: 10 January 2018 | Accepted: 12 January 2018

DOI: 10.1002/aoc.4305

FULL PAPER

WILEY Applied Organometallic Chemistry

Synthesis, molecular geometry, spectroscopic studies and thermal properties of Co(II) complexes

Sh.M. Morgan[1] | M.A. Diab[2] | A.Z. El-Sonbati[2]

[1] Environmental Monitoring Laboratory, Ministry of Health, Port Said, Egypt

[2] Chemistry Department, Faculty of Science, Damietta University, Damietta, Egypt

Correspondence
Sh.M. Morgan, Environmental Monitoring Laboratory, Ministry of Health, Port Said, Egypt.
Email: shimaa_mohamad2010@yahoo.com

Co(II) complexes **(1-4)** were prepared and characterized by elemental analyses, infrared spectra, spectral studies, magnetic susceptibility measurements, X-ray diffraction analysis and thermogravimetric analysis (TGA). The X-ray diffraction patterns of Co(II) complexes were observed many peaks which indicate the polycrystalline nature. The thermodynamic parameters were calculated by using Coats–Redfern and Horowitz–Metzger methods. The bond length, bond angle and quantum chemical parameters of the Co(II) complexes were studied and discussed. The Co(II) complexes were tested against various Gram-positive bacteria, Gram-negative bacteria and fungi. It was found that the Co(II) complex **(1)** has more antifungal activity than miconazole (antifungal standard drug) against *P. italicum* at all concentration. The Co(II) complex (**2**) has more antibacterial activity than the penicillin against *K. pneumoniae* at all concentration. The interaction between Co(II) complexes and calf thymus DNA show hypochromism effect. The relationship between the values of HOMO–LUMO energy gap (ΔE) and the values of intrinsic binding constant (K_b) is revealed increasing of HOMO–LUMO energy gap accompanied by the decrease of K_b.

KEYWORDS
biological activity, Co(II) complexes, quantum chemical parameters, thermal analysis, thermodynamics parameters

1 | INTRODUCTION

Coordination chemistry and biochemistry of rhodanine and its derivatives have attracted increased interest due to their chelating ability and their pharmacological applications.[1–3] The pharmacological activity is found to be more in the case of complexes when compared to the free ligand and some side effects may decrease upon complexation. Rhodanine azo dyes compounds are one of the most prevalent ligands in coordination chemistry. In addition to important roles in metal extracting agents,[4] solar cells[5,6] and biosensors.[7] Because of the optical properties of azo dye compounds, one of the most important applications of azo compounds is in the optical data storage. The metal complexes of azo dye compounds have a variety of biological and medicinal applications.[8]

Rhodanine azo dyes and some of its derivatives are important in the coordination chemistry, which makes them strong ligands in coordination compounds.[9–12] Azo dyes act as bidentate, tridentate and/or tetradentate donor and coordinate with transition metal ions to form complexes. Rhodanine azo compounds contain hetero atoms which are considered to be centers of adsorption (oxygen, nitrogen and sulfur) and could be utilized as anti- corrosion agents for protection of metals.[13]

The metal coordination to biologically active molecules can be used to enhance their antimicrobial activity; therefore, many studies on the interaction between rhodanine azo ligands with several metal ions have been

reported.[9,14–16] The interaction of metal ions with rhodanine azo ligands becomes an increasingly important field due to the antibacterial properties of the resulting complexes.

The present study describes the preparation of Co(II) complexes and characterized by elemental analyses, infrared spectra, spectral studies, magnetic susceptibility measurements, molar conductance measurements, X-ray diffraction analysis and thermal analysis. Calf thymus DNA binding of the complexes is studied by absorption spectroscopy. The optimized structural geometry and quantum chemical parameters such as highest occupied molecular orbital energy, the lowest unoccupied molecular orbital energy and HOMO–LUMO energy gap were also discussed. Biological activity of the complexes was evaluated against Gram positive bacterial species, Gram negative bacterial species and fungal species.

2 | EXPERIMENTAL

2.1 | Material and reagents

2-Thioxothiazolidin-4-one, aniline or *p*-derivatives of aniline were purchased from Aldrich Chemical Co., Inc. $Co(CH_3COO)_2 . 4H_2O$ (Sigma Aldrich). The solvents as dimethylformamide (DMF), dimethylsulfoxide (DMSO) and ethanol were bought from BDH. The calf thymus DNA (CT-DNA) was acquired from SRL (India).

2.2 | Analytical and physical measurements

Elemental microanalyses of the complexes for C, H, N and S were analyzed in the Microanalytical Center, Cairo University, Egypt. Infrared spectra are recorded using Perkin-Elmer 1340 spectrophotometer. Thermal analysis was computed on Simultaneous Thermal Analyzer (STA) 6000 system using thermogravimetric analysis method and the samples were analyzed at the heating rate of 10 °C/min under dynamic nitrogen atmosphere in the temperature range from 30 to 800 °C. X-Ray diffraction analysis of complexes was recorded on X-ray diffractometer analysis in the range of diffraction angle $2\theta^o = 4–80^o$ with Cu $K_{\alpha 1}$-radiation. The applied voltage and the tube current are 40 kV and 30 mA, respectively. The diffraction peaks in powder spectra are indexed and the lattice parameters are determined with the aid of CRYSFIRE computer program.[17] The value of interplanar spacing and Miller indices for each diffraction peak are determined by using CHEKCELL program.[18–20] Mass spectrum was recorded using MS-5988 GS-MS Hewlett-Packard by the EI technique at 70 eV. The conductance measurement was achieved using Sargent Welch Scientific Co., Skokie, IL, USA. The magnetic moment of the complexes was determined using the Gouy's method at room temperature. Magnetic moments were computed utilizing the equation, $\mu_{eff.} = 2.84\ [Tc_M{}^{coor.}]^{1/2}$.

2.3 | Computational method

Molecular structures of the complexes were optimized by HF technique with 3-21G basis set. ChemBio Draw and optimized utilizing Perkin Elmer ChemBio3D software.[21,22]

Docking calculations for ligands were carried out on receptors of the androgen receptor prostate cancer mutant H874Y ligand binding domain bound with testosterone and a TIF2 box3 coactivator peptide 740-753 (Protein Data Bank (PDB) code: 2Q7L Hormone) and crystal structure of the BRCT repeat region from the breast cancer associated protein, BRCA1 (Protein Data Bank (PDB) code: 1JNX Gene regulation).[21]

Statistical analysis data are statistically analysed for variance were carried out by SPSS software version 17 and the least significant difference (LSD) at 0.05 level using one-way analysis of variance (ANOVA).

2.4 | Methodology of antibacterial and antifungal activity

The method of agar well diffusion was adopted for this examination.[23,24] The antifungal activities of the investigated compounds are scanned against four local fungal types (*Penicillium italicum*, *Alternaria alternata*, *Aspergillus niger* and *Fusarium oxysporium*) on DOX agar medium and the antibacterial activities are scanned on nutrient agar medium against two local Gram positive bacterial types (*Staphylococcus aureus* and *Bacillus cereus)* and two local Gram negative bacterial (*Escherichia coli* and *Klebsiella pneumoniae*). The concentrations of every solution of complex were 50, 100 and 150 μg/ml in dimethylformamide (DMF). Utilizing a sterile cork borer (10 mm diameter), wells was made in medium of agar plates previously seeded with the test microorganism. 200 μL of every complex was applied in every well. The agar plates were kept at 4 °C for at least 30 min to allow the diffusion of the complex to agar medium. The plates were then incubated at 37 °C or 30 °C for bacteria and fungi, respectively. The diameters of inhibition zone were specified after 24 hour and 7 days for bacteria and fungi, respectively, taking the consideration of the control values (DMF). The biological activity of the complexes was compared with standard drugs such as penicillin (antibacterial standard drug) and miconazole (antifungal standard drug).

2.5 | DNA binding experiments

The binding properties of Co(II) complexes to Calf thymus DNA (CT-DNA) are studied using electronic absorption spectroscopy.[24,25] Electronic absorption spectra are carried out using 1 cm quartz cuvette at room temperature by fixing the concentration of complex (1×10^{-3} mol L^{-1}) while progressively increasing the concentration of calf thymus DNA (CT-DNA). The intrinsic binding constant (K_b) of the complexes with calf thymus DNA was determined[24,25]:

$$[DNA]/(\epsilon_a - \epsilon_f) = [DNA]/(\epsilon_b - \epsilon_f) + 1/K_b(\epsilon_a - \epsilon_f) \quad (1)$$

where ϵ_a is the molar extinction coefficient observed for the A_{obs}/[complex] at the given DNA concentration, ϵ_f is the molar extinction coefficient of the free complex in solution, [DNA] is the concentration of CT-DNA in base pairs and ϵ_b is the molar extinction coefficient of the complex when fully bond to DNA.

2.6 | Preparation of Co(II) complexes

5-(4-Arylazo)-2-thioxothiazolidin-4-one ligands (HL_n) were synthesized and characterized by the well established standard method as reported in literatures.[9,10,23] To an ethanolic solution of ligands, a solution of $Co(CH_3COO)_2.4H_2O$ in ethanol was added and the mixture was refluxed on a water bath for ~ 6-8 hrs. The solid complexes were separated by filtration and washed thoroughly with ethanol and diethyl ether and dried in a vacuum desiccators over anhydrous $CaCl_2$. The data of elemental analyses suggested that the formulae of the prepared complexes as $[Co(L_n)(O_2CCH_3)(OH_2)_2]$ mH_2O (Table S1) according to the following equation:

$$HL_n + Co(CH_3COO)_2.4H_2O \rightarrow [Co(L_n)(O_2CCH_3)(OH_2)_2]\ mH_2O + CH_3COOH$$

where L_n = deprotonated HL_n and m is the number of the water molecules.

It is interesting to point out that, the data of elemental analysis are in satisfactory agreement with the expected formula which gives support for the suggested composition. The composition coordination mode and geometry of the Co(II) complexes were established on the basis of elemental analyses, infrared spectra, conductivity measurements, magnetic properties and thermal analysis.

2.7 | $[Co(L_1)(O_2CCH_3)(OH_2)_2]$ $2H_2O$ (1)

Microanalysis for $C_{12}H_{19}N_3O_8S_2Co$ (455.933); Found: C, 31.36; H, 3.09; N, 8.96; S, 13.89; Co, 12.59%. Calculated C, 31.58; H, 3.29; N, 9.21; S, 14.04; Co, 12.93%, in agreement with the formula of the complex used for thermogravimetric analysis (TGA) (below-mentioned). Yield 66%, grayish brown, m.p. > 300 °C. IR spectra: 1564 cm^{-1} (CH_3COO^- sym.), 1442 cm^{-1} (CH_3COO^- asym.), 3330 cm^{-1} (OH water), 460 cm^{-1} (O-Co), 445 cm^{-1} (N-Co). Molar conductance (10^{-3} M, DMSO): 4.5 Ω^{-1} cm^2 mol^{-1}. $\mu_{eff.}$ = 5.31 B.M., UV.vis.: Electronic spectrum: 9300 ($^4T_{1g}(F) \rightarrow {}^4T_{2g}(F)(\upsilon_1)$) and 18180 cm^{-1} ($^4T_{1g}(F) \rightarrow {}^4T_{1g}(P)(\upsilon_3)$) transitions. Electronic parameters; $\beta = 0.592$, $\upsilon_3/\upsilon_1 = 1.96$; LFSE (kcal mol^{-1}) = 29.70.

2.8 | $[Co(L_2)(O_2CCH_3)(OH_2)_2]$ H_2O (2)

Microanalysis for $C_{12}H_{17}N_3O_6S_2Co$ (421.933); Found: C, 33.92; H, 3.36; N, 9.86; S, 14.80; Co, 13.69%. Calculated C, 34.13; H, 3.56; N, 9.95; S, 15.17; Co, 13.97%, in agreement with the formula of the complex used for thermogravimetric analysis (TGA) (below-mentioned). Yield 71%, dark brown, m.p. > 300 °C. IR spectra: 1564 cm^{-1} (CH_3COO^- sym.), 1423 cm^{-1} (CH_3COO^- asym.), 3403 cm^{-1} (OH water), 510 cm^{-1} (O-Co), 460 cm^{-1} (N-Co). Molar conductance (10^{-3} M, DMSO): 5.5 Ω^{-1} cm^2 mol^{-1}. $\mu_{eff.}$ = 4.86 B.M.

2.9 | $[Co(L_3)(O_2CCH_3)(OH_2)_2]$ $\frac{1}{2}H_2O$ (3)

Microanalysis for $C_{11}H_{14}N_3O_{5.5}S_2Co$ (398.933); Found: C, 32.88; H, 3.09; N, 10.31; S, 15.87; Co, 14.79%. Calculated C, 33.09; H, 3.26; N, 10.53; S, 16.04; Co, 14.77%, in agreement with the formula of the complex used for thermogravimetric analysis (TGA) (below-mentioned). Yield 76%, pale brown, m.p. > 300 °C. Mass spectrum, the ion of m/z = 398.933 (m/z = 266.933, 251.933, 91 and 77 by losing 2.5 H_2O, + $C_3H_3O_3$, NH, C_2S_2NCo and N atoms, respectively). IR spectra: 1564 cm^{-1} (CH_3COO^- sym.), 1439 cm^{-1} (CH_3COO^- asym.), 3434 cm^{-1} (OH water), 525 cm^{-1} (O-Co), 470 cm^{-1} (N-Co). Molar conductance (10^{-3} M, DMSO): 6.5 Ω^{-1} cm^2 mol^{-1}. $\mu_{eff.}$ = 4.88 B.M., UV. vis.): Electronic spectrum: 9100 ($^4T_{1g}(F) \rightarrow {}^4T_{2g}(F)(\upsilon_1)$) and 18500 cm^{-1} ($^4T_{1g}(F) \rightarrow {}^4T_{1g}(P)(\upsilon_3)$) transitions. Electronic parameters; $\beta = 0.624$, $\upsilon_3/\upsilon_1 = 2.03$; LFSE (kcal mol^{-1}) = 29.18.

2.10 | $[Co(L_4)(O_2CCH_3)(OH_2)_2]$ $2H_2O$ (4)

Microanalysis for $C_{11}H_{16}N_4O_9S_2Co$ (470.933); Found: C, 27.85; H, 2.35; N, 11.72; S, 13.25; Co, 12.48%. Calculated C, 28.03; H, 2.55; N, 11.89; S, 13.59; Co, 12.51%, in agreement with the formula of the complex used for thermogravimetric analysis (TGA) (below-mentioned). Yield 81%, brown, m.p. > 300 °C. IR spectra: 1564 cm^{-1} (CH_3COO^- sym.), 1446 cm^{-1} (CH_3COO^- asym.), 3326 cm^{-1} (OH water), 540 cm^{-1} (O-Co), 478 cm^{-1} (N-Co). Molar

conductance (10^{-3} M, DMSO): 7.4 Ω^{-1} cm^2 mol^{-1}. $\mu_{eff.}$ = 4.81 B.M., UV.vis.: Electronic spectrum: 8700 ($^4T_{1g}(F) \rightarrow {}^4T_{2g}(F)(\upsilon_1)$) and 17750 cm^{-1} ($^4T_{1g}(F) \rightarrow {}^4T_{1g}(P)(\upsilon_3)$) transitions. Electronic parameters; β =0.471, υ_3/υ_1= 2.04; LFSE (kcal mol^{-1}) = 21.65.

3 | RESULTS AND DISCUSSION

3.1 | Molecular docking study of the ligands

Affinity of molecules to anticancer receptors is very important in drug design. Therefore, we carried out molecular docking of the tautomeric forms (A-C) of ligands (HL_n) with different anticancer receptors target such as; prostate cancer (PDB code: 2Q7L) and breast cancer (PDB code: 1JNX) through AutoDock server and the interaction curves are shown in Figures S1 and S2. Tables S2 and S3 show the bending of tautomeric forms (A-C) of ligands (HL_n) and some parameters with the selected anticancer receptors and the interaction sites through a hydrogen bond. The interaction energies values by kcal/mol are also tabulated. The more value with negative charge is the most stable interaction. The 2D plot curves of binding for tautomeric forms (A-C) of ligands (HL_n) with the selected anticancer receptors are shown in Figure S3 and S4, appear bending interaction sites of tautomeric forms (A-C) of ligands (HL_n) with proteins active sites of receptors. Figure S3 and S4 reveal that 1JNX receptor cannot be formed hydrogen bond with hetero atoms of tautomeric forms (A-C) of ligands (HL_n) except HL_1 (forms B and C), HL_3 (form C) and HL_4 (form A) as well as 2Q7L receptor can be formed hydrogen bond depending on active site of protein receptor and all tautomeric forms (A-C) of ligands (HL_n). The HB plot curves which explain these interactions of tautomeric forms (A-C) of ligands (HL_n) are shown in Figure S5 and S6. Free estimated free energy of binding, estimated inhibition constant (K_i) and interact surface area reveal the most favored binding. The ligand has more negative value of estimated free energy of binding and the higher value of estimated inhibition constant (K_i) is the more efficient binding. The obtained data showed a best binding between the tautomeric forms (A-C) of ligands (HL_n) and the receptor of prostate cancer (PDB code: 2Q7L) than the receptor of breast cancer (PDB code: 1JNX) (Tables S2 and S3), so, it is possible to used the ligands (HL_n) for cancer treatment due to the ability to interact with anticancer receptors.

3.2 | Characterization of Co(II) complexes

The analytical data are in good agreement with the composition of Co(II) complexes and showing that the complexes have 1:1 (metal:ligand) stoichiometry of the type $[Co(L_n)(O_2CCH_3)(OH_2)_2]$ mH_2O where L_n and CH_3COO^- act as bidentate ligands (Scheme 1). All Co(II) complexes are soluble in dimethylformamide (DMF) and dimethylsulfoxide (DMSO), stable in air and high melting point. The molar conductance of the Co(II) complexes solutions in DMSO (10^{-3} M) at room temperature was measured. The molar conductivity values are in the range of 4.5-7.4 Ω^{-1} cm^2 mol^{-1}, which indicate a non-conducting nature and there is no counter ion present outside the coordination sphere of cobalt complexes.[24] The favorable coordinating character of acetate gives a chance for their inclusion inside the coordination sphere with one central atom.

The mass spectrum of complex **(3)** is characterized by moderate to high relative an intensity molecular ions peaks at 70 eV (Figure 1). The fragmentation pattern of complex **(3)** shows a molecular ion peak at m/z 398.933 which is corresponding to the formula weight of the complex $[Co(L_3)(O_2CCH_3)(OH_2)_2]$ ½H_2O **(3)**. Clearly, the molecular ion peaks are in good concurrence with their suggested empirical formula as indicated from elemental analyses. The spectrum shows base molecular ion peak at m/z 266.933 corresponding to the structure **I** ($CoC_8H_6N_3S_2$) as shown in Scheme 2. The peak at m/z

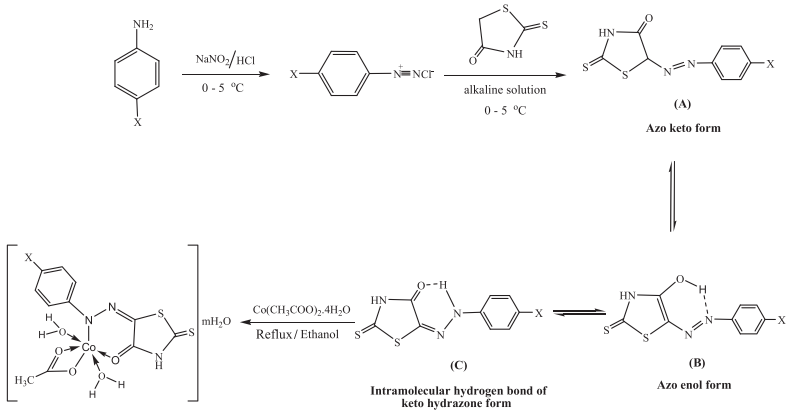

SCHEME 1 The formation mechanism of the Co(II) complexes

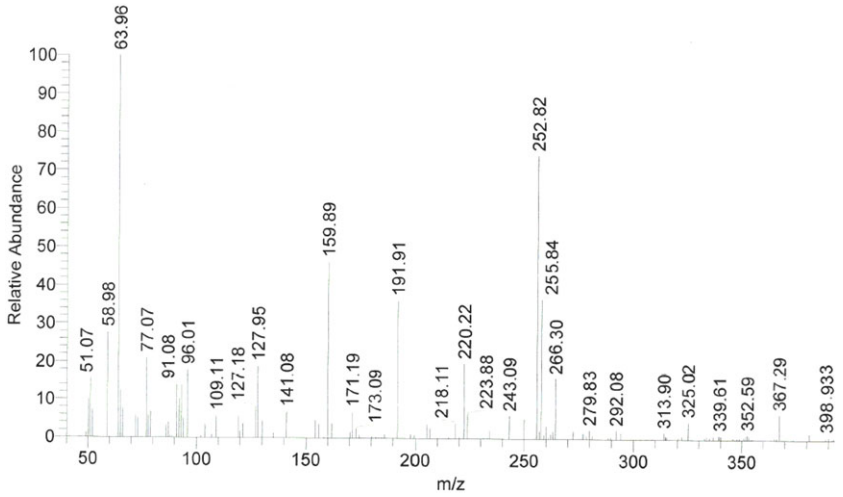

FIGURE 1 Mass spectrum of complex **(3)**

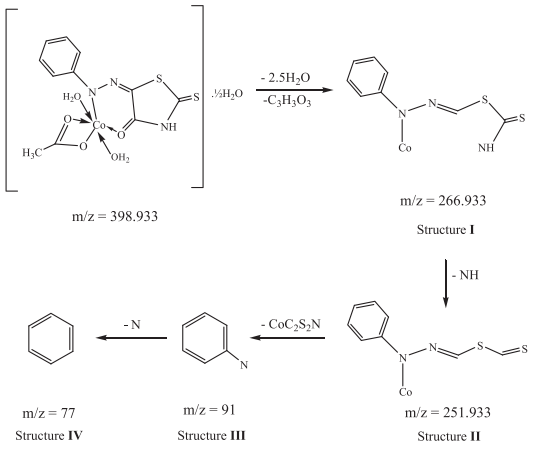

SCHEME 2 Fragmentation patterns of complex **(3)**

251.933 is due to the structure **II** ($CoC_8H_5N_2S_2$). The peaks observed at m/z 91 and 77 corresponding to structures **III** and **IV** (C_6H_5N and C_6H_5), respectively. The fragmentation mass spectrum of complex **(3)** is in good agreement with the proposed composition.

3.3 | IR analysis study

The IR spectra of HL_n display vibrations at ~ 3180-3040, 1725-1755, 1130-1140, ~1640 and 820-880 cm^{-1} assigned to asymmetric and symmetric stretching vibrations of NH group and intramolecular hydrogen bonding NH...O systems (Scheme 1C), show two intense carbonyl bands [υ(C=O...H), υ(C=O)] consistent with a keto hydrazone form (Scheme 1C), six-membered intramolecular bonding according to El-Sonbati *et al.*,[9] assigned to υ(N-N) vibrations mode,[26] is attributed to υ(C=N-) structure through resonating phenomena and this has been confirmed by a number of previous published data of keto hydrazone analogous and υ(CS), respectively. Overlapping in some bands belonging to aggregated neighboring groups contributing to H-migration may commensurate the presence of tautomer form (keto hydrazone).[9,23] The hydrazone form of the ligands contributed to mononuclear complexes as monobasic bidentate mode. The three structural forms were give best orientation for donor atoms to verify the coordination mode (Scheme 1).

The mode of coordination proposed for all the Co(II) complexes is based on literature data for related systems and the following observations:

i. In complexes **(1-4)** band in the range of 3480-3530 cm^{-1} is observed. These regions are due to different probabilities: (a) it is due to either free OH/NH, (b) bonded –OH group or –NH group or (c) due to the presence of coordinated water molecules.
ii. In Co(II) complexes, the absence any peak due to the (=N-NH) moiety, implies that the ligands exist in tautomeric equilibrium [(Scheme 1 (A↔C)]. The tautomeric form losses hydrazone proton when complexes with metal acetate as mononegative chelating agents.
iii. Lower frequencies of υ(CO) by 45-30 cm^{-1} on going from ligands can be assigned to binding of the carbonyl group (which has an electron- withdrawing nature) to the Co(II) ion *via* its lone pair of electrons which will lead to a decrease of the electron-withdrawing effect of carbonyl group and hence affects the position of the carbonyl band in the spectra of the complexes. This shift can be also be accounted for the hydrogen bond formation with the outer sphere ligands.
iv. The strong band due to υ(N-N) vibration modes affected on complexation and it is blue shifted and appeared as a weak bands.
v. In all complexes, it is confirmed that the ligands are coordinated to the Co(II) ion as a monobasic bidentate, coordinating *via* the oxygen of the

carbonyl group of rhodanine (M-O) and the proton displacement from hydrazone (=N-NH) group (M-N) through Co(II) ion occurs.

vi. The coordination of bidentate acetate group is indicated by the appearance of two additional bands due to $\upsilon_s(COO^-)$ and $\upsilon_{as}(COO^-)$, and the magnitude of $\Delta\upsilon = \upsilon_{as}(COO^-) - \upsilon_s(COO^-) = \sim 118\text{-}141\ cm^{-1}$.[27]

vii. A broad stretching vibration bands in the region of 3440-3310 cm^{-1} in all Co(II) complexes which can be accounted for by the presence of hydrated and/or coordinated water molecules.[9,19,28]

3.4 | Molecular geometry study

Molecular geometry and quantum chemical parameters of Co(II) complexes were calculated theoretically and recorded in Table 1 where geometries structures were optimized and drawn using Perkin Elmer ChemBio3D software.[24] From Table 1, keto hydrazone structure **(I)** of Co(II) complexes have smaller HOMO–LUMO energy gap (ΔE) values which give indication that the keto hydrazone structure **(I)** is more stable than azo enol structure **(II)** (Figure 2). The molecular geometry of keto hydrazone structure **(I)** of Co(II) complexes are shown in Figure 3. It is found that the computed net charges on active centers is N(8) and O(10) for keto hydrazone structure **(I)** and is the most negative charges than azo enol structure **(II)** which that makes it react more with the metal ion. In our present study, the corresponding bond lengths of C(1)-C(2) and C(2)-O(10) are found in the range 1.364-1.366 Å and 1.261-1.263 Å, respectively. These values are lesser than the rhodanine molecule due to the attachment of *p*-aniline derivatives.[9] On the other hand, the C-C bond length (C(11)-C(18), C(18)-C(19), C(19)-C(20), C(20)-C(21), C(21)-C(22) and C(22)-C(11)) of six-membered rings are relatively in the range 1.337-1.359 Å (Tables S4-S7). The bond angles of N(3)-C(4)-S(5), N(3)-C(4)-S(6), S(5)-C(4)-S(6), C(4)-S(5)-C(1), C(1)-C(2)-N(3), N(3)-C(2)-O(10), C(1)-C(2)-O(10) and Co(9)-O(10)-C(2) are found in the range 101.672-102.723°, 130.256-129.860°, 127.395-128.017°, 92.608-93.678°, 103.557-104.029°, 111.386-112.556°, 143.846-144.393° and 111.217-111.473°, respectively.

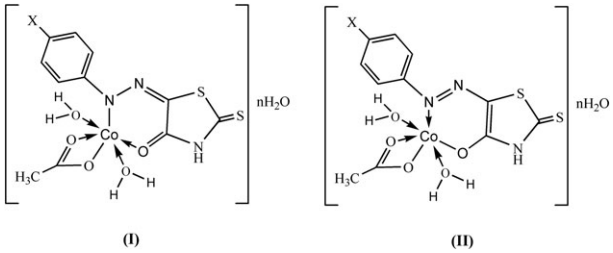

FIGURE 2 Structures of Co(II) complexes [keto hydrazone structure **(I)** and azo enol structure **(II)**]

The HOMO and LUMO orbital's for keto hydrazone structure **(I)** of Co(II) complexes are shown in Figure 4. Quantum chemical parameters of the Co(II) complexes are calculated[24]:

$$\Delta E = E_{LUMO} - E_{HOMO} \tag{2}$$

$$\chi = \frac{-(E_{HOMO} + E_{LUMO})}{2} \tag{3}$$

$$\eta = \frac{E_{LUMO} - E_{HOMO}}{2} \tag{4}$$

$$\sigma = 1/\eta \tag{5}$$

$$Pi = -\chi \tag{6}$$

$$S = \frac{1}{2\eta} \tag{7}$$

$$\Delta N_{max} = -Pi/\eta \tag{8}$$

where E_{HOMO} is the highest occupied molecular orbital energy, E_{LUMO} is the lowest unoccupied molecular orbital energy, χ is the absolute electronegativities, η is the absolute hardness, σ is the absolute softness, Pi is the chemical potential, S is the global softness and ΔN_{max} is the additional electronic charge.

TABLE 1 The calculated quantum chemical parameters of Co(II) complexes [keto hydrazone structure **(I)** and azo enol structure **(II)**]

Structure	Complex[a]	E_{HOMO} (eV)	E_{LUMO} (eV)	ΔE (eV)	χ (eV)	η (eV)	σ $(eV)^{-1}$	Pi (eV)	S $(eV)^{-1}$	ΔN_{max}
Keto hydrazone **(I)**	**(1)**	-1.574	-1.300	0.274	1.437	0.137	7.299	-1.437	3.649	10.489
	(2)	-1.693	-1.372	0.321	1.533	0.161	6.231	-1.533	3.115	9.548
	(3)	-1.798	-0.938	0.860	1.368	0.430	2.326	-1.368	1.163	3.181
	(4)	-3.703	-1.468	2.235	2.586	1.118	0.895	-2.586	0.447	2.314
Azo enol **(II)**	**(1)**	-1.754	-0.918	0.836	1.336	0.418	2.392	-1.336	1.196	3.196
	(2)	-1.370	-0.608	0.762	0.989	0.381	2.625	-0.989	1.312	2.596
	(3)	-1.802	-0.920	0.882	1.361	0.441	2.268	-1.361	1.134	3.086
	(4)	-4.074	-1.501	2.573	2.788	1.287	0.777	-2.788	0.389	2.167

[a]The number corresponds to that used in Section 2.

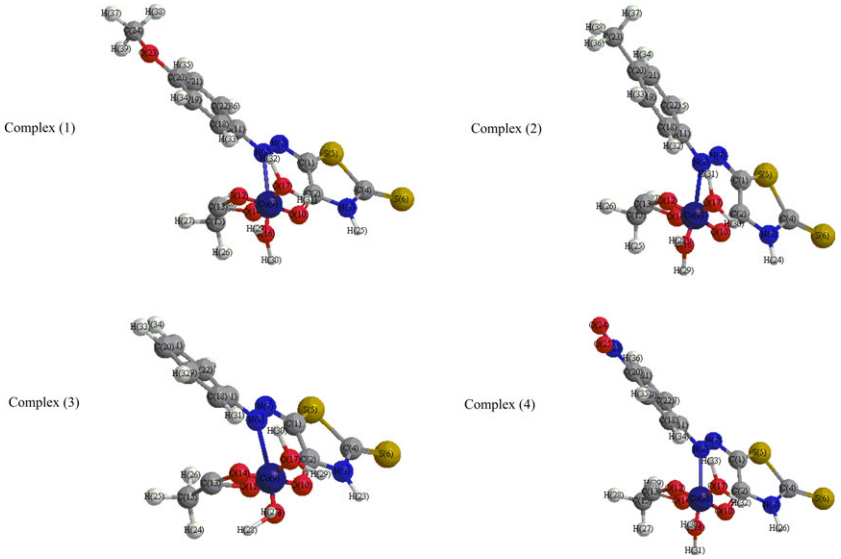

FIGURE 3 The optimized structural geometry of Co(II) complexes

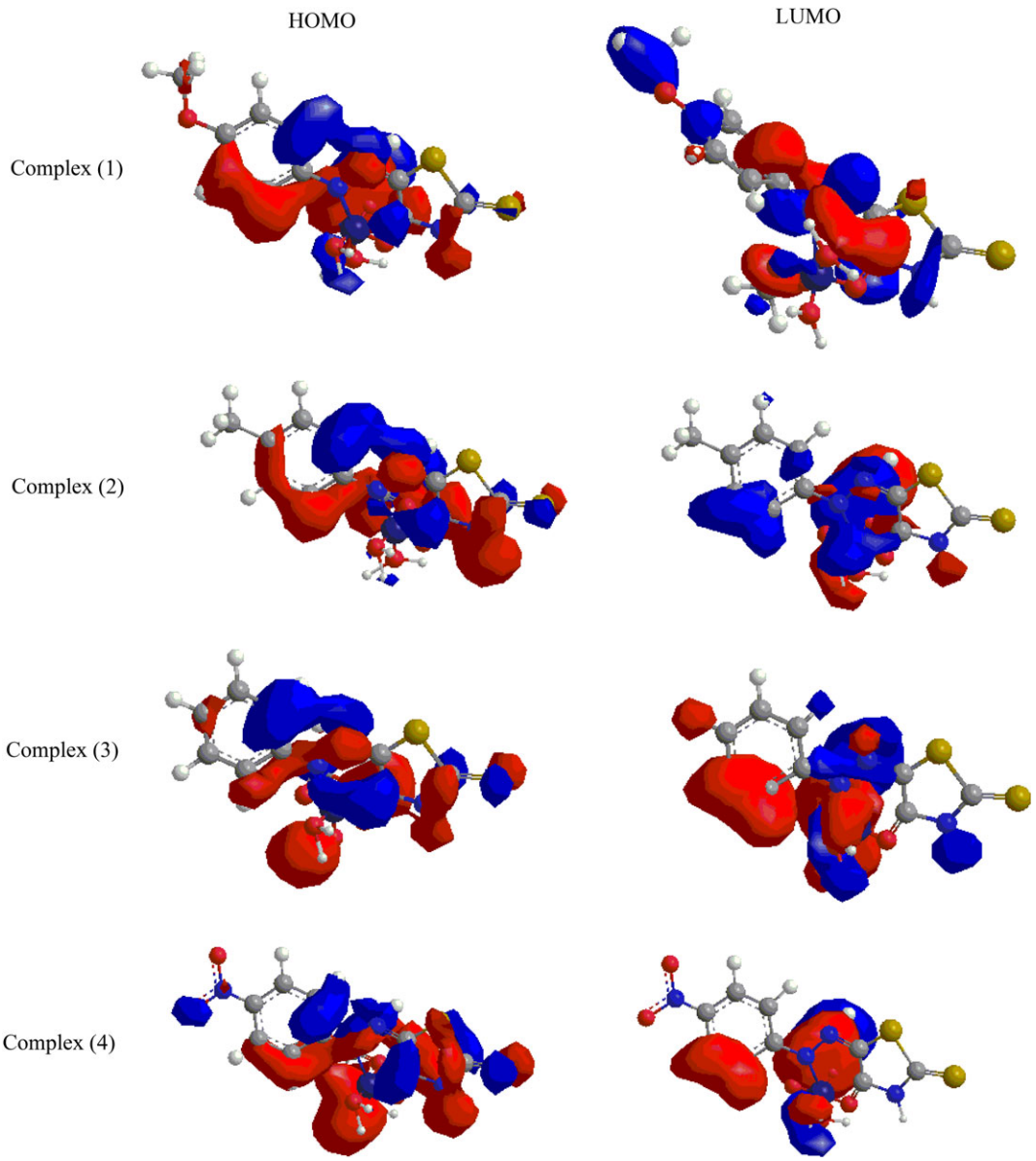

FIGURE 4 Molecular structures (HOMO and LUMO) of Co(II) complexes

The order of the HOMO–LUMO energy gap (ΔE) values was found to be **(1)** < **(2)** < **(3)** < **(4)**. The positive electrophilicity index (χ) value and the negative chemical potential (Pi) value indicated that the molecules of the complexes capable of accepting electrons from the environment and its energy must decrease upon accepting electronic charge.

3.5 | Magnetic susceptibility measurements

The magnetic moments of the cobalt(II) complexes are given in Table 2. The values of magnetic moment at room temperature, attributed to three unpaired electrons. The magnetic susceptibilities of these complexes fall in the range 4.81-5.31 B.M. acceptable for octahedral cobalt(II). One of the interesting features of these data is the small variation in the magnetic moment among the various ligand complexes. This is probably an indication that the donor atoms in the ligand predominant in their effect on the metalloelement due to the electron nature of the substituent.

3.6 | Electronic spectral study

The cobalt(II) complexes show two electronic spectral bands at ~ 8700 – 9300 cm^{-1} ($^4T_{1g}(F) \rightarrow {}^4T_{2g}(F)(\upsilon_1)$) and ~ 17750 – 18500 cm^{-1} ($^4T_{1g}(F) \rightarrow {}^4T_{1g}(P)(\upsilon_3)$) transitions, corresponding to a six-coordinated geometry of an octahedral cobalt(II) complexes. The υ_3/υ_1 ratio for Co(II) complexes occur in the range of 1.96-2.04. The value for the majority of octahedral cobalt(II) complexes is 1.95-2.48.[29]

Various ligand field parameters are calculated for the cobalt(II) complexes on the basis of electronic spectral and listed in Table 2. The ligand field parameters show that the complexes possess an octahedral symmetry with strong covalent bond.[30] The ligand field stabilization energies (LFSE) and interelectronic repulsion parameter are calculated.[24,29] The nephelauzetic parameter (β) values lie in the range of 0.471 – 0.624. These values indicate the appreciable covalent character of metal ligand 'sigma' bond. The value of B` is lower than the free ion, this is because of the orbital overlap and delocalization of d-orbital. The order of the Dq values among these cobalt(II) complexes was found to be **(4)** < **(3)** < **(1)**.

3.7 | X-ray diffraction analysis study

Single crystals of Co(II) complexes could not be prepared to get the X-ray diffraction (XRD) and hence the powder diffraction data were obtained for structural characterization. Structure determination by X-ray powder diffraction data has gone through a recent surge since it has become important to get to the structural information of materials, which do not yield good quality single crystals.

X-ray diffraction analysis patterns of Co(II) complexes are shown in Figure 5. Many peaks are observed and indicate the polycrystalline nature of Co(II) complexes **(2-4)**. The average size of the crystal (ζ) can be calculated using by Debye-Scherrer equation[24]:

$$\xi = \frac{k\lambda}{\beta_{1/2}\cos\theta} \tag{9}$$

where k is the constant equal to 0.95 for organic compounds,[19,31] θ is the Bragg's angle, λ is the X-ray wavelength (1.540598 Å) and $\beta_{1/2}$ is the width measured in radians of the half maximum peak intensity. The value of dislocation density (δ) which is the number of dislocation lines per unit area of the crystal, can be calculated from the average crystallite size (ζ) and calculated according to the relation[19,24]:

$$\delta = \frac{1}{\xi^2} \tag{10}$$

The value of ζ is 32.37, 27.32 and 29.17 nm for complexes **(2-4)**, respectively. The dislocation density values (δ) are 9.54×10^{-4}, 1.34×10^{-3} and 1.18×10^{-3} nm^{-2} for complexes **(2-4)**, respectively.

The optimum Miller indices (*hkl*) and lattice parameters a, b, c, α, β and γ for the investigated complexes is determined by CHEKCELL software.[17,32] The calculated crystal system of complex **(3)** is found to be monoclinic with space group P2/m. The estimated lattice parameters are found to be 90.00°, 90.54°, 90.00°, 20.9576 Å, 4.0728 Å and 11.8809 Å, for α, β, γ, a, b and c, respectively. The calculated crystal system of complex

TABLE 2 Electronic parameters of the Co(II) complexes

Complex[a]	$\mu_{eff.}$ (B.M.)	υ_3/υ_1	Bands (cm^{-1})	Dq (cm^{-1})	B` (cm^{-1})	β	β° %	LFSE (kcal mol^{-1})	Dq/ B`
(1)	5.31	1.96	9300,18180	1037	663	0.592	40.80	29.70	1.56
(3)	4.88	2.03	9100, 18500	1019	699	0.624	37.60	29.18	1.46
(4)	4.81	2.04	8700, 17750	756	527	0.471	52.90	21.65	1.43

[a]The number corresponds to that used in Section 2.

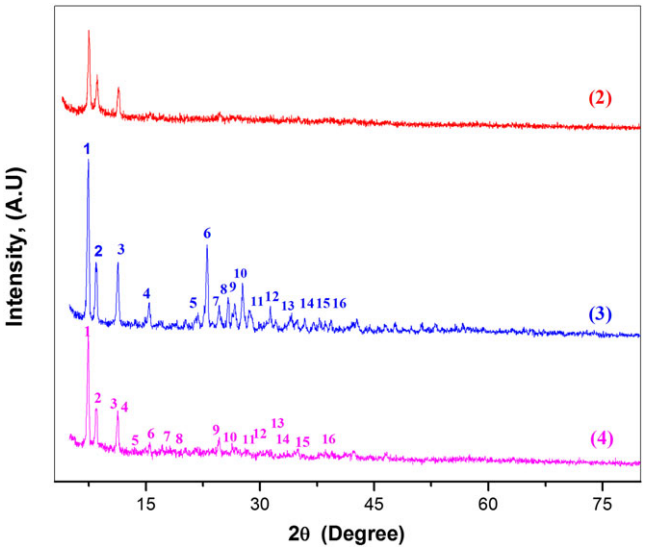

FIGURE 5 X-ray diffraction patterns of Co(II) complexes

(4) is found to be monoclinic with space group P21/c. The estimated lattice parameters are found to be 90.00°, 91.04°, 90.00°, 23.6900 Å, 20.6990 Å and 3.8280 Å, for α, β, γ, a, b and c, respectively. The inter-planar spacing, d, and Miller indices, *hkl*, which estimated by CRYSFIRE are recorded in Tables 3 and 4.

3.8 | Biological activity study

Antibacterial activity and antifungal activity of Co(II) complexes were tested against Gram positive bacteria as *Staphylococcus aureus* and *Bacillus cereus* and Gram negative bacteria as *Escherichia coli* and *Klebsiella pneumoniae* and fungi species as *Aspergillus niger*, *Fusarium oxysporium*, *Penicillium italicum* and *Alternaria alternata*. The antimicrobial activities data showed in Tables 5 and 6.

Co(II) complexes **(1)** and **(4)** have antibacterial activity against *E. coli* while complex **(2)** showed antibacterial activity against *K. pneumoniae* and have no antibacterial activity against *S. aureus* and *B. cereus*. It is found that the complex **(1)** is more effective than the other complexes against *E. coli* (Figure 6). As well as the complex **(1)** has more antibacterial activity than the penicillin against *E. coli* at low concentration (50 μg/ml) (Table 5). Complex **(2)** has effective than the other complexes against *K. pneumoniae* and more active than the penicillin against *K. pneumoniae* for all concentration.

Also, Co(II) complexes **(1-4)** have no antifungal activity against *Alternaria alternata, Fusarium oxysporium* and *Aspergillus niger*.[33] Complexes **(1-3)** have antifungal activity against *Penicillium italicum* (Table 6). Co(II) complex **(1)** is more activity of antifungal than miconazole (standard drug) against P. *italicum* at all concentration (Figure 7).

3.9 | Calf thymus DNA binding study

DNA is the primary pharmacological target of antitumor drugs and therefore, it is essential to explore the interactions of molecule with DNA. The binding mode and propensity of the complexes to Calf thymus DNA

TABLE 3 The lattice parameters and Miller indices of complex **(3)**

Peak no.	$2\theta_{obs.}$ (°)	$d_{obs.}$ (Å)	$2\theta_{calc.}$ (°)	$d_{calc.}$ (Å)	h k l
1	7.4126	11.9164	7.4351	11.8804	001
2	8.4697	10.4313	8.4316	10.4784	200
3	11.3041	7.8213	11.3029	7.8222	201
4	15.4130	5.7443	15.4540	5.7291	$\bar{1}02$
5	21.7847	4.0764	21.8044	4.0728	010
6	23.0286	3.859	23.0667	4.8527	011
7	24.6323	3.6112	24.5747	3.6196	$\bar{2}11$
8	25.8205	3.4477	25.8800	3.4399	$\bar{5}02$
9	26.6510	3.3421	26.6479	3.3425	601
10	27.7146	3.2162	27.7210	3.2155	$\bar{4}10$
11	28.6908	3.1090	28.6968	3.1083	$\bar{4}11$
12	31.3458	2.8514	31.3563	2.8505	204
13	34.0666	2.6297	34.0384	2.6318	$\bar{6}03$
14	35.8651	2.5018	35.8429	2.5033	$\bar{4}13$
15	37.8533	2.3748	37.8331	2.3761	005
16	39.3267	2.2892	39.3284	2.2891	$\bar{9}01$

TABLE 4 The lattice parameters and Miller indices for complex **(4)**

Peak no.	$2\theta_{obs.}$ (°)	$d_{obs.}$ (Å)	$2\theta_{calc.}$ (°)	$d_{calc.}$ (Å)	h k l
1	7.4188	11.9064	7.4532	11.8516	200
2	8.5009	10.3931	8.5197	10.3702	020
3	11.2981	7.8255	11.3288	7.8043	$\bar{2}20$
4	11.9406	7.4058	11.977	7.3834	$\bar{3}10$
5	14.9398	5.9251	14.9382	5.9258	400
6	15.4925	5.7150	15.5396	5.6978	$\bar{4}10$
7	17.1115	5.1777	17.0871	5.1851	040
8	18.6356	4.7576	18.6642	4.7503	$\bar{2}40$
9	24.6367	3.6106	24.6626	3.6069	$\bar{2}11$
10	26.3465	3.3800	26.2981	3.3862	700
11	29.0946	3.0667	29.0911	3.0671	331
12	30.0413	2.9722	30.0252	2.9738	$\bar{5}11$
13	31.2470	2.8602	31.2414	2.8607	$\bar{6}50$
14	31.4642	2.8409	31.4687	2.8406	521
15	34.9370	2.5661	34.9332	2.5664	541
16	38.6342	2.3286	38.6189	2.3295	171

TABLE 5 The results of antibacterial activity for Co(II) complexes and recorded as the average diameter of inhibition zone (mm) ± standard error

	Conc. (μg/ml)	Gram positive bacteria		Gram negative bacteria	
Complex[a]		*Bacillus cereus*	*Staphylococcus aureus*	*Escherichia coli*	*Klebsiella pneumoniae*
(1)	50	-ve	-ve	4 ± 0 *	-ve
	100	-ve	-ve	3 ± 0.2	-ve
	150	-ve	-ve	3 ± 0.2	-ve
(2)	50	-ve	-ve	-ve	3 ± 0.1 *
	100	-ve	-ve	-ve	3 ± 0.1 *
	150	-ve	-ve	-ve	3 ± 0 *
(3)	50	-ve	-ve	2 ± 0.1	-ve
	100	-ve	-ve	-ve	-ve
	150	-ve	-ve	-ve	-ve
(4)	50	-ve	-ve	3 ± 0.1	-ve
	100	-ve	-ve	2 ± 0	-ve
	150	-ve	-ve	2 ± 0	-ve
Penicillin	50	1 ± 0.1	2 ± 0	1± 0	-ve
	100	3 ± 0.2	2 ± 0.1	3 ± 0	-ve
	150	3 ± 0.1	2 ± 0	3 ± 0	-ve

[a]The number corresponds to that used in Section 2.

*Indicate significant different value from that of penicillin.

determines the potential of these complexes to act as chemotherapeutic agents. Electronic absorption spectroscopy is one of the most universally employed methods to study the binding modes and binding extent of compounds to DNA. DNA usually exhibits hypochromism as a consequence of the intercalation mode, which involves a strong stacking interaction between an aromatic chromophore and the base pairs of DNA.[34–36] This strong stacking interaction is due to the contraction of calf thymus (CT)-DNA in the helix axis and its conformational changes.[37,38]

The intrinsic binding constant to CT-DNA for Co(II) complexes is determine by absorption spectra (UV-Visible spectroscopy). The absorption spectra of all

TABLE 6 The results of antifungal activity for Co(II) complexes and recorded as the average diameter of inhibition zone (mm) ± standard error

Complex[a]	Conc. (μg/ml)	*Aspergillus niger*	*Fusarium oxysporum*	*Alternaria alternata*	*Penicillium italicum*
(1)	50	-ve	-ve	-ve	2 ± 0 *
	100	-ve	-ve	-ve	7 ± 0.2 *
	150	-ve	-ve	-ve	5 ± 0.1 *
(2)	50	-ve	-ve	-ve	-ve
	100	-ve	-ve	-ve	-ve
	150	-ve	-ve	-ve	5 ± 0.2 *
(3)	50	-ve	-ve	-ve	1 ± 0
	100	-ve	-ve	-ve	1 ± 0
	150	-ve	-ve	-ve	1 ± 0
(4)	50	-ve	-ve	-ve	-ve
	100	-ve	-ve	-ve	-ve
	150	-ve	-ve	-ve	-ve
Miconazole	50	1 ± 0	2 ± 0	5 ± 0	1 ± 0
	100	3 ± 0.1	3 ± 0	6 ± 0	1 ± 0
	150	4 ± 0	3 ± 0	6 ± 0.1	2 ± 0

[a]The number corresponds to that used in Section 2.

*Indicate significant different value from that of miconazole.

Co(II) complexes decrease gradually with increasing concentration of CT-DNA in the range 300-580 nm (Figure S7) and show hypochromism effect with slight bathochromic shift (~1–2 nm).[20,39] The plots of [DNA]/(ϵ_a–ϵ_f) versus [DNA] and the intrinsic binding constant (K_b) was given by the ratio of the slope to the intercept. The K_b value of complexes **(1)**, **(2)**, **(3)** and **(4)** was determined by equation 1 and found to be 6.57 x 10^4, 6.05 x 10^4, 4.30 x 10^4 and 2.85 x 10^4 M^{-1}, respectively. The intrinsic binding constant values (K_b) of complexes were increased according to the following order: **(1)** > **(2)** > **(3)** > **(4)**.

The calculated energies of the Frontier orbital's, lowest unoccupied (E_{LUMO}) and highest occupied molecular orbital's (E_{HOMO}) (ΔE (eV) = E_{LUMO}–E_{HOMO}) of Co(II) complexes are correlated with the values of intrinsic binding constant (K_b). The relationship between ΔE and K_b of Co(II) complexes reveals increasing of ΔE accompanied by the decrease of the intrinsic binding constant values (K_b) as shown in Figure 8.

3.10 | Thermal analysis and thermodynamic parameters studies

The thermal analysis of Co(II) complexes were characterized on the basis of thermogravimetric analysis (TGA) method in the temperature range 30–800 °C as shown in Figure 9. The TGA curves are taken as a proof for the existing of water molecules in outside of the coordination sphere and/or coordinated water molecules as well as the anions to be coordination sphere in complexes. The intervals of temperature and the percentage of loss of mass of Co(II) complexes are listed in Table 7. The experimental weight loss values for the Co(II) complexes are in good agreement with the calculated values.

The first mass loss for complex **(1)** occurs in the range of 45-120 °C, corresponding to loss of two water molecules in outside of the coordination sphere with an observed mass loss of 7.60% (calcd. = 7.89%). The second decomposition step takes place within the range of 120-410 °C attributed to the loss of two coordinated water molecules, one coordinated acetate group and $C_3HN_2S_2$ with 48.28% (calcd. = 49.13%). The last decomposition step occurs at 410-800 °C is assigned to loss of C_5H_7NO with a weight loss 20.87% (calcd. = 22.28%). The CoO and carbon atoms are the final products remaining.

For complex **(2)**, the first step appears in the temperature range of 45-81 °C attributed to the loss of one water molecule in outside of the coordination sphere with mass loss 4.46% (calcd. = 4.27%).[19] The second step occurs in the temperature range of 81-440 °C attributed to loss of two coordinated water molecules, one coordinated acetate group and C_2S_2NH with mass loss 47.22% (calcd. = 46.93%). The third step of decomposition in the temperature range of 440-800 °C assigned to loss of $C_5H_7N_2$ with mass loss 21.48% (calcd. = 22.50%). The final residue is cobalt oxide + 3C atoms, and the experimental result (26.84%) is in good agreement with the result of theoretical calculation (26.30%).

Complex **(3)** shows a first decomposition stage in the range of 45-95 °C assignable to the loss of ½H_2O molecule

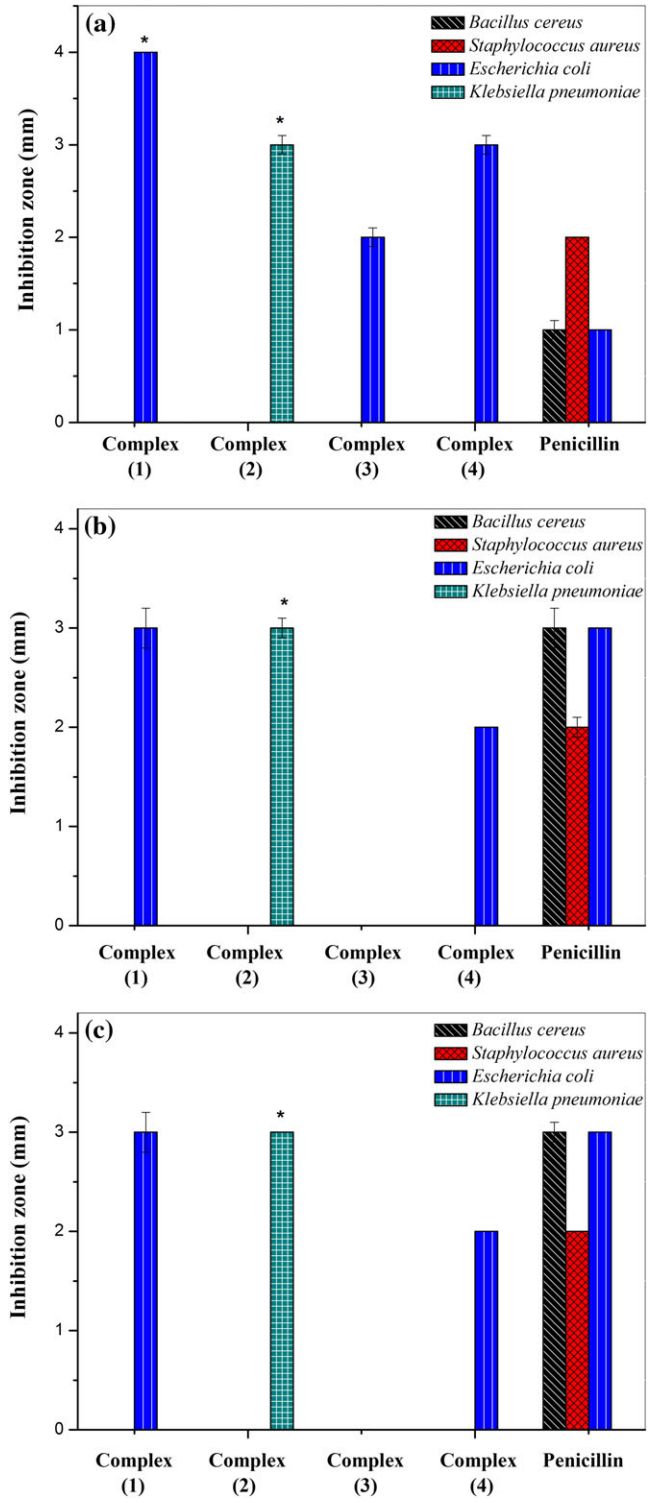

FIGURE 6 Histogram of the antibacterial activity of Co(II) complexes at a) 50, b) 100 and c) 150 μg/ml. The inhibition zone is on record as mm ± standard error. * Indicate significant different value from that of penicillin

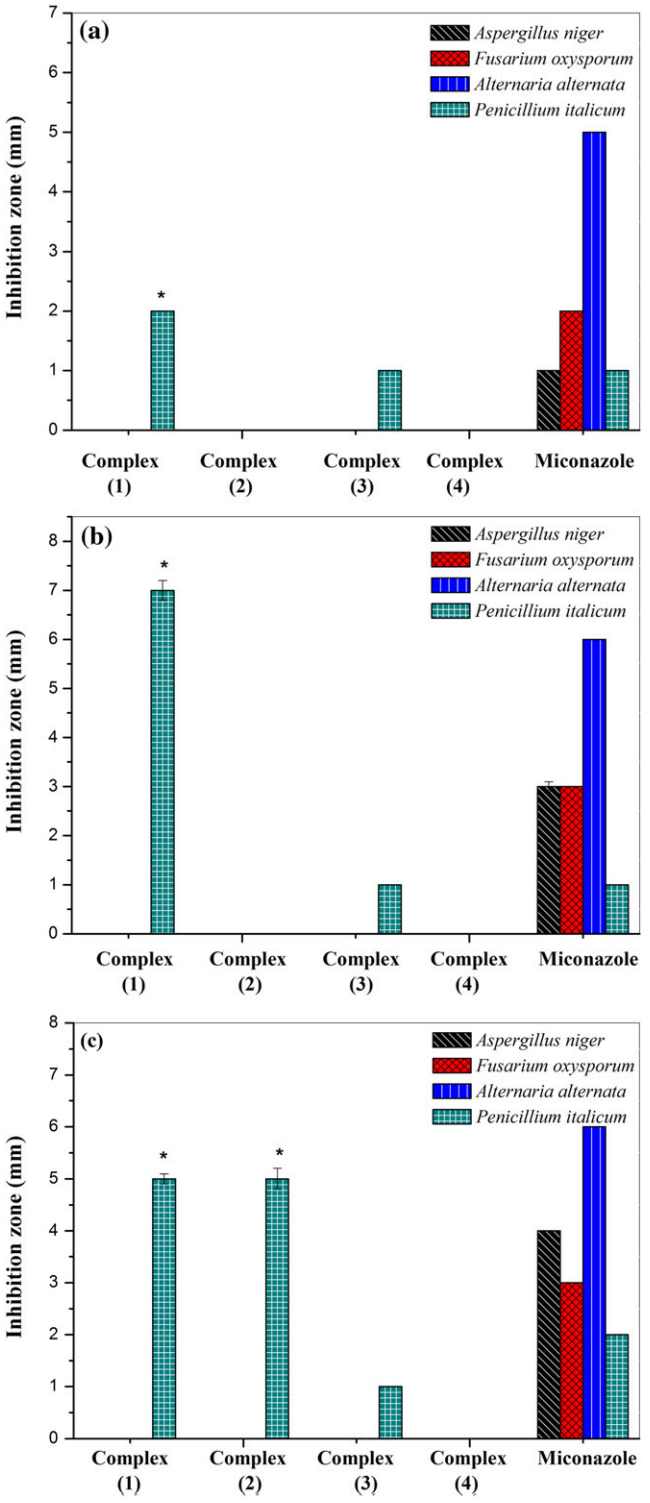

FIGURE 7 Histogram of the antifungal activity of Co(II) complexes at a) 50, b) 100 and c) 150 μg/ml. The inhibition zone is on record as mm ± standard error. * indicate significant different value from that of miconazole

in outside of the coordination sphere with mass loss 2.02% (calcd. = 2.26%). The second stage of decomposition in the temperature range of 95-250 °C is attributed to loss of two coordinated water molecules, one coordinated acetate group and C_2S_2 with mass loss 44.74% (calcd. = 45.87%). The final stage at 250-800 °C involves thermal degradation of the part of the ligand ($C_4H_6N_3$) with an estimated mass loss of 24.63% (calcd. = 24.06%) leaving is cobalt

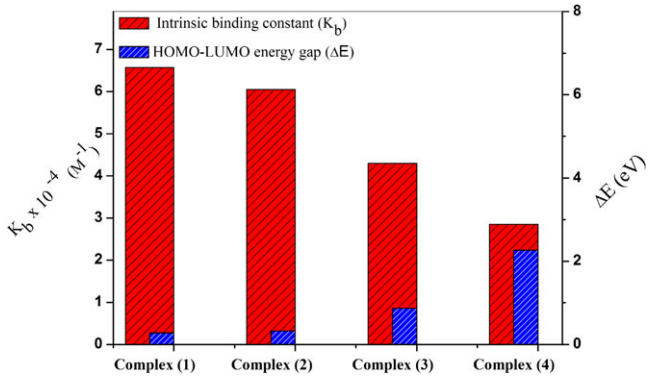

FIGURE 8 Histogram of HOMO–LUMO energy gap (ΔE) (eV) and intrinsic binding constant (K_b) (M^{-1}) of Co(II) complexes

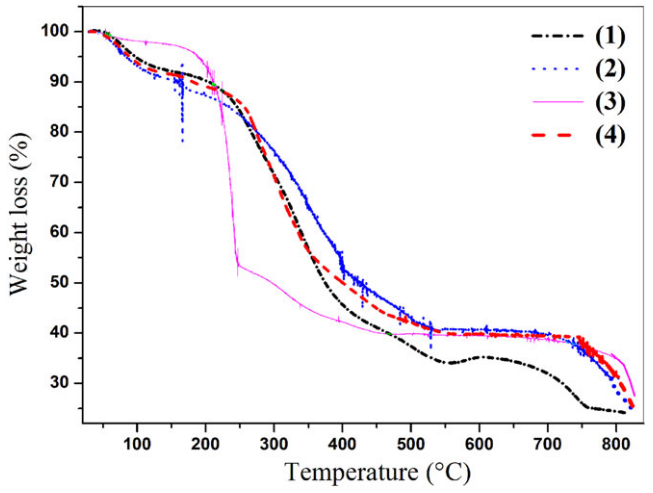

FIGURE 9 TGA thermal analysis of Co(II) complexes

oxide + 3C atoms as final residual component with 28.61% (calcd. = 27.81%).

For complex **(4)**, the first step at 45-110 °C is assigned to the loss of two water molecules in outside of the coordination sphere with mass loss 7.11% (calcd. = 7.64%). The second step at 110-410 °C corresponds to the loss of two coordinated water molecules, one coordinated acetate group and $C_2S_2N_2$ with mass loss 44.69% (calcd. = 44.82%). The third step at 410-800 °C corresponds to the thermal decomposition of the ligand ($C_4H_5N_2O_2$) with mass loss of 24.01% (calcd. = 23.99%) and formation of cobalt oxide as a metallic residue and contaminated 3C atoms amounting to 24.19% (calcd. = 23.55%).

The thermodynamic studies upon the thermal degradation processes are a powerful indication to provide sufficient knowledge about thermal activation energy of decomposition (E_a), enthalpy (ΔH^*), entropy (ΔS^*) and Gibbs free energy change of the decomposition (ΔG^*). From TG curves, Coast-Redfern and Horowitz-Metzger methods[40,41] are employed to calculate mentioned thermodynamic parameters (Figure 10 and 11).

Enthalpy (ΔH^*) is calculated from $\Delta H^* = E_a - RT$ and Gibbs free energy of decomposition (ΔG^*) is calculated from $\Delta G^* = \Delta H^* - T\,\Delta S^*$. The calculated values of E_a, ΔS^*, ΔH^* and ΔG^* for Co(II) complexes are recorded in Table 8. The calculated thermodynamic from the two methods of Coast-Redfern and Horowitz-Metzger are suitable agreement with each other.[19,42,43] From the calculated data can be pointed the following:

TABLE 7 TGA thermal analysis data of Co(II) complexes

Complex[a]	Temp. range (°C)	Found mass loss (calcd.) %	Assignment
(1)	45-120	7.60 (7.89)	Loss of $2H_2O$ molecules in outside of the coordination sphere
	120-410	48.28 (49.13)	Loss of two coordinated water molecules, coordinated CH_3COO group and $C_3HN_2S_2$
	410-800	20.87 (22.28)	Loss of C_5H_7NO
	> 800	23.25 (21.70)	CoO + 2 carbon atoms
(2)	45-81	4.46 (4.27)	Loss of H_2O molecule in outside of the coordination sphere
	81-440	47.22 (46.93)	Loss of two coordinated water molecules, coordinated CH_3COO group and C_2S_2NH
	440-800	21.48 (22.50)	Loss of $C_5H_7N_2$
	> 800	26.84 (26.30)	CoO + 3 carbon atoms
(3)	40-95	2.02 (2.26)	Loss of ½H_2O molecule in outside of the coordination sphere
	95-250	44.74 (45.87)	Loss of two coordinated water molecules, coordinated CH_3COO group and C_2S_2
	250-800	24.63 (24.06)	Loss of $C_4H_6N_3$
	> 800	28.61 (27.81)	CoO + 3 carbon atoms
(4)	45-110	7.11 (7.64)	Loss of $2H_2O$ molecules in outside of the coordination sphere
	110-410	44.69 (44.82)	Loss of two coordinated water molecules, coordinated CH_3COO group and $C_2S_2N_2$
	410-800	24.01 (23.99)	Loss of $C_4H_5N_2O_2$
	> 800	24.19 (23.55)	CoO + 3 carbon atoms

[a]The number corresponds to that used in Section 2.

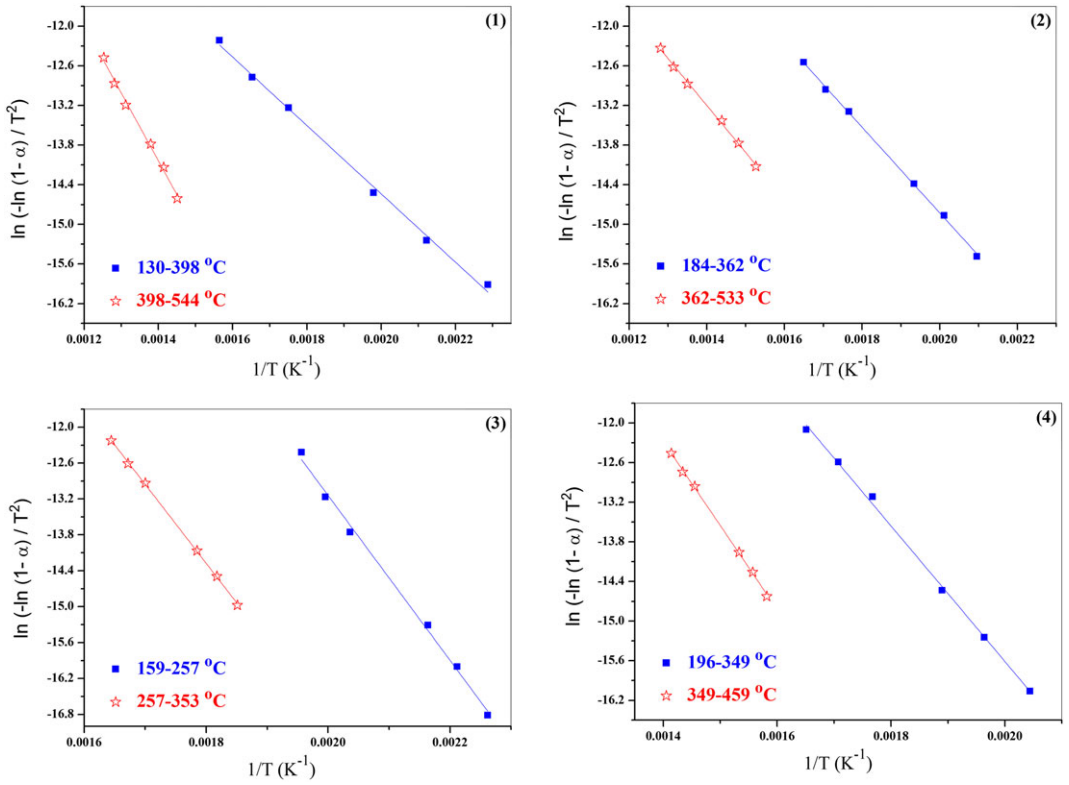

FIGURE 10 Coats–Redfern method of Co(II) complexes

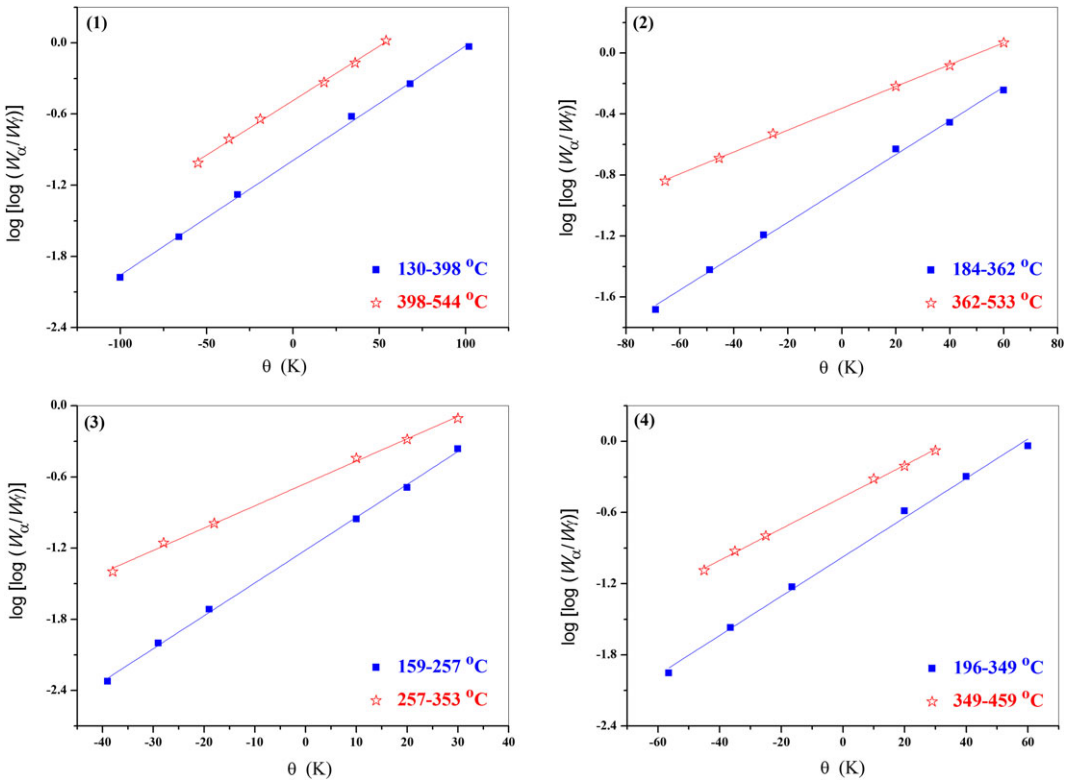

FIGURE 11 Horowitz-Metzger method of Co(II) complexes

1. Entropy (ΔS^*) is found to be of negative values for Co(II) complexes indicate more ordered activated complex than the reactants or the reaction is slow.[24]
2. According to the values of the thermal activation energy of decomposition (E_a), the order of E_a value of the Co(II) complexes is **(3)** > **(4)** > **(2)** > **(1)**. The

TABLE 8 Thermodynamic parameters of Co(II) complexes

Complex[a]	Decomposition temperature (°C)	Method	Thermodynamic parameters				Correlation coefficient (r)
			E_a (kJ mol^{-1})	ΔS^* (J mol^{-1} K^{-1})	ΔH^* (kJ mol^{-1})	ΔG^* (kJ mol^{-1})	
(1)	130-398	CR	43.0	-229	38.5	161	0.99626
		HM	53.3	-197	48.8	155	0.99855
	398-544	CR	85.4	-188	79.2	219	0.99469
		HM	97.4	-169	91.3	217	0.99064
(2)	184-362	CR	53.9	-204	49.4	161	0.99909
		HM	63.4	-176	58.9	155	0.99762
	362-533	CR	59.2	-217	53.2	210	0.99760
		HM	71.1	-199	65.1	209	0.99931
(3)	159-257	CR	107	-77.0	103	139	0.99567
		HM	115	-39.8	111	130	0.99872
	257-353	CR	110	-104	105	165	0.99960
		HM	120	-79.8	116	162	0.99784
(4)	196-349	CR	85.3	-144	80.8	159	0.99795
		HM	94.4	-116	89.9	153	0.99601
	349-459	CR	106	-139	100	194	0.99911
		HM	117	-119	112	192	0.99865

[a]The number corresponds to that used in Section 2.

complex is high value of E_a confirms that the high stability.[9]

3. The positive values of Gibbs free energy of decomposition (ΔG^*) confirm that the process is non-spontaneous.

4 | CONCLUSIONS

In this paper, the preparation of Co(II) complexes were reported. Elemental analyses, IR spectra, spectral analyses, conductivity measurements and magnetic properties results used to confirm the stoichiometry and formulation of the complexes. The detailed thermal study played an important role to confirm the number and nature of water molecules in coordination complexes. IR spectra show that the ligands act as monobasic bidentate ligands by coordinating *via* the nitrogen atom of the deprotonated –NH group and the carbonyl group and forming a six-membered chelating ring. The calculated crystal system of complexes **(3)** and **(4)** is found to be monoclinic with space group P2/m and monoclinic with space group P21/c, respectively. Co(II) complexes were tested against bacteria and fungi species. Complex **(1)** has good antibacterial and antifungal activities against *Escherichia coli* and *Penicillium italicum*, respectively.

ACKNOWLEDGEMENT

Authors wish to express thanks Prof. Dr. M.I. Abou-Dobara, Botany Department, Damietta University, Egypt for his help during testing antimicrobial activity.

ORCID

Sh.M. Morgan http://orcid.org/0000-0002-8921-4894
M.A. Diab http://orcid.org/0000-0002-9042-1356
A.Z. El-Sonbati http://orcid.org/0000-0001-7059-966X

REFERENCES

[1] B. T. Moorthy, S. Ravi, M. Srivastava, K. K. Chiruvella, H. Hemlal, O. Joy, S. C. Raghavan, *Bioorg. Med. Chem. Lett.* **2010**, *20*, 6297.

[2] M. Sortino, P. Delgado, S. Juárez, J. Quiroga, R. Abonía, B. Insuasty, M. Nogueras, L. Rodero, F. M. Garibotto, R. D. Enriz, S. A. Zacchino, *Bioorg. Med. Chem.* **2007**, *15*, 484.

[3] N. S. Cutshall, C. O'Day, M. Prezhdo, *Bioorg. Med. Chem. Lett.* **2005**, *15*, 3374.

[4] W. I. Stephen, A. Townshend, *Anal. Chim. Acta* **1965**, *33*, 257.

[5] X. Qian, L. Lu, Y.-Z. Zhu, H.-H. Gao, J.-Y. Zheng, *Dyes Pigm.* **2015**, *113*, 737.

[6] Q. Fan, M. Li, P. Yang, Y. Liu, M. Xiao, X. Wang, H. Tan, Y. Wang, R. Yang, W. Zhu, *Dyes Pigm.* **2015**, *116*, 13.

[7] J. Yu, L. Ge, P. Dai, S. Ge, S. Liu, *Biosens. Bioelectron.* **2010**, *25*, 2065.

[8] G. Galan Alfonso, J. L. Gomez Ariza, *Microchem. J.* **1981**, *26*, 574.

[9] A. Z. El-Sonbati, M. A. Diab, Sh. M. Morgan, *J. Mol. Liq.* **2017**, *225*, 195.

[10] A. Z. El-Sonbati, A. A. M. Belal, M. S. El-Gharib, Sh. M. Morgan, *Spectrochim. Acta A* **2012**, *95*, 627.

[11] A. Z. El-Sonbati, M. A. Diab, A. A. M. Belal, Sh. M. Morgan, *Spectrochim. Acta A* **2012**, *99*, 353.

[12] N. A. El-Ghamaz, A. Z. El-Sonbati, Sh. M. Morgan, *J. Mol. Struct.* **2012**, *1027*, 92.

[13] A. M. Eldesoky, M. A. El-Bindary, A. Z. El-Sonbati, Sh. M. Morgan, *J. Mater. Environ. Sci.* **2015**, *6*, 2260.

[14] A. Z. El-Sonbati, A. A. M. Belal, M. A. Diab, M. Z. Balboula, *Spectrochim. Acta A* **2011**, *78*, 1119.

[15] A. Z. El-Sonbati, M. A. Diab, M. M. El-Halawany, N. E. Salam, *Spectrochim. Acta A* **2010**, *77*, 755.

[16] Sh. M. Morgan, N. A. El-Ghamaz, M. A. Diab, *J. Mol. Struct.* **2018**, https://doi.org/10.1016/j.molstruc.2018.01.079.

[17] R. Shirley, *The CRYSFIRE system for Automatic Powder Indexing: User's Manual*, the Lattice Press, Guildford **2000**.

[18] J. Laugier, B. Bochu, *LMGP-suite suite of programs for the interpretation of X-ray experiments*, ENSP/Laboratoire des Materiaux et du Genie Physique, Saint Martin d'Heres **2000**.

[19] N. A. El-Ghamaz, M. A. Diab, A. Z. El-Sonbati, Sh. M. Morgan, O. L. Salem, *Chem. Pap.* **2017**, *71*, 2417.

[20] Sh. M. Morgan, A. Z. El-Sonbati, M. A. El-Mogazy, *Appl. Organomet. Chem.* **2018**, https://doi.org/10.1002/aoc.4264.

[21] H. M. Refaat, H. A. El-Badway, Sh. M. Morgan, *J. Mol. Liq.* **2016**, *220*, 802.

[22] G. G. Mohamed, A. A. El-Sherif, M. A. Saad, S. E. A. El-Sawy, Sh. M. Morgan, *J. Mol. Liq.* **2016**, *223*, 1311.

[23] M. I. Abou-Dobara, A. Z. El-Sonbati, S. M. Morgan, *World J. Microbiol. Biotechnol.* **2013**, *29*, 119.

[24] Sh. M. Morgan, A. Z. El-Sonbati, H. R. Eissa, *J. Mol. Liq.* **2017**, *240*, 752.

[25] L. H. Abdel-Rahman, R. M. El-Khatib, L. A. E. Nassr, A. M. Abu-Dief, *J. Mol. Struct.* **2013**, *1040*, 9.

[26] A. Z. El-Sonbati, M. A. Diab, M. S. El-Shehawy, M. Moqbel, *Spectrochim. Acta A* **2010**, *75*, 394.

[27] K. Nakamoto, *Infrared and Raman Spectra of Inorganic and Coordination Compounds*, Wiley Interscience Publication, John Wiley & Sons Inc., New York **1986**.

[28] Sh. M. Morgan, M. A. Diab, A. Z. El-Sonbati, *Appl. Organomet. Chem.* **2018**, https://doi.org/10.1002/aoc.4281.

[29] A. P. B. Lever, *Inorganic and electronic spectroscopy*, first ed., Elsevier, Amsterdam **1968**.

[30] A. Z. El-Sonbati, M. A. Diab, R. H. Mohamed, *Polym. Int.* **2011**, *60*, 1467.

[31] A. Z. El-Sonbati, M. A. Diab, A. A. El-Bindary, A. M. Eldesoky, Sh. M. Morgan, *Spectrochim. Acta A.* **2015**, *135*, 774.

[32] M. M. Makhlouf, H. M. Zeyada, *Synth. Met.* **2016**, *211*, 1.

[33] N. S. Habib, S. M. Rida, E. A. M. Badawey, H. T. Y. Fahmy, H. A. Ghozlan, *Eur. J. Med. Chem.* **1997**, *32*, 759.

[34] L. M. Wu, H. B. Ten, X. B. Ke, W. J. Xu, J. T. Su, S. C. Liang, X. M. Hu, *Chem. Biodivers.* **2007**, *4*, 2198.

[35] A. Rompel, H. Fischer, D. Meiwes, K. B. Karentzopoulos, R. Dillinger, F. Tuczek, H. Witzel, B. Krebs, *J. Biol. Inorg. Chem.* **1999**, *4*, 56.

[36] C. Gokce, R. Gup, *Chem. Pap.* **2013**, *67*, 1293.

[37] S. Rajalakshmi, T. Weyhermuller, A. J. Freddy, H. R. Vasanthi, B. U. Nair, *Eur. J. Med. Chem.* **2011**, *46*, 608.

[38] N. Hassan, A. Z. El-Sonbati, M. G. El-Desouky, *J. Mol. Liq.* **2017**, *242*, 293.

[39] A. Z. El-Sonbati, M. A. Diab, Sh. M. Morgan, H. A. Seyam, *J. Mol. Struct.* **2018**, *1154*, 354.

[40] A. W. Coats, J. P. Redfern, *Nature* **1964**, *201*, 68.

[41] H. H. Horowitz, G. Metzger, *Anal. Chem.* **1963**, *35*, 1464.

[42] A. Z. El-Sonbati, M. A. Diab, Sh. M. Morgan, M. Z. Balboula, *Appl. Organomet. Chem.* **2017**, https://doi.org/10.1002/aoc.4059.

[43] A. Z. El-Sonbati, M. A. Diab, Sh. M. Morgan, A. M. Eldesoky, M. Z. Balboula, *Appl. Organomet. Chem.* https://doi.org/10.1002/aoc.4207.

SUPPORTING INFORMATION

Additional Supporting Information may be found online in the supporting information tab for this article.

How to cite this article: Morgan ShM, Diab MA, El-Sonbati AZ. Synthesis, molecular geometry, spectroscopic studies and thermal properties of Co(II) complexes. *Appl Organometal Chem*. 2018; e4305. https://doi.org/10.1002/aoc.4305